

Multiplicity-dependent p_T distributions of identified particles in pp collisions at 7 TeV within the HIJING/ $B\bar{B}$ v2.0 model

V. Topor Pop^{1,2} and M. Petrovici^{2,*}¹Physics Department, McGill University, Montreal H3A 2T8, Canada²National Institute for Physics and Nuclear Engineering-Horia Hulubei Hadron Physics Department R-077125, Bucharest, Romania

(Received 4 June 2018; revised manuscript received 25 August 2018; published 10 December 2018)

Effects of strong longitudinal color fields (SLCF) on the identified (anti)particle transverse momentum (p_T) distributions in pp collision at $\sqrt{s} = 7$ TeV are investigated within the framework of the HIJING/ $B\bar{B}$ v2.0 model. The comparison with the experiment is performed in terms of the correlation between mean transverse momentum ($\langle p_T \rangle$) and multiplicity (N_{ch}^*) of charged particles at central rapidity, as well as the ratios of the p_T distributions to the one corresponding to the minimum bias (MB) pp collisions at the same energy, each of them normalized to the corresponding charged particle density, for high multiplicity (HM, $N_{\text{ch}} > 100$) and low multiplicity (LM, $N_{\text{ch}} < 100$) class of events. The theoretical calculations show that an increase of the strength of color fields (as characterized by the effective values of the string tension κ), from $\kappa = 2$ to $\kappa = 5$ GeV/fm, from LM to HM class of events, respectively, led to a ratio at low and intermediate p_T (i.e., $1 \text{ GeV}/c < p_T < 6 \text{ GeV}/c$), consistent with recent data obtained at the Large Hadron Collider by the ALICE Collaboration. These results point out the necessity of introducing a multiplicity (or energy density) dependence for the effective value of the string tension. Moreover, the string tension $\kappa = 5$ GeV/fm, describing the p_T spectra of identified particles (anti)particle in pp collisions at $\sqrt{s} = 7$ TeV for high charged particle (HM) multiplicity event classes, has the same value as the one used in describing the p_T spectra in central Pb-Pb collisions at $\sqrt{s_{NN}} = 2.76$ TeV. Therefore, we can conclude that at the LHC energies the global features of the interactions could be mostly determined by the properties of the initial chromoelectric flux tubes, while the system size may play a minor role.

DOI: [10.1103/PhysRevC.98.064903](https://doi.org/10.1103/PhysRevC.98.064903)

I. INTRODUCTION

Relativistic and ultrarelativistic heavy-ion experimental data evidenced global features such as flow, baryon-meson anomaly, (multi)strange enhancement, and jet quenching, which support the interpretation of theoretical (phenomenological) models as signature of deconfined, strongly interacting thermalized phase, called quark-gluon plasma (sQGP). In contrast, similar effects were not observed in proton-proton (pp) and proton-nucleus (p - A) collisions and these results have been considered of interest only as reference data for nucleus-nucleus (A - A) collisions. Features reminiscent from heavy-ion phenomenology have been recently evidenced in such reactions at the Large Hadron Collider (LHC) energies, i.e., long-range near-side ridge in particle correlations [1–4], collective flow [5–7], or strangeness enhancement [8] observed in high charged particle multiplicity events. The nature of these similarities is still an open question. Do they

originate from a deconfined phase following a hydrodynamic evolution like in nucleus-nucleus (A - A) collisions or are they a consequence of the initial state dynamics manifested in the final-state observables [5,9–11]? Most probably the two processes coexist, with a dense thermalized central core and an outer corona. Such a picture is successfully implemented in the energy-sharing parton-based theory with off-shell remnants and ladder splitting (EPOS) model [12–14]. The core-corona interplay in the light flavor hadron production for Pb-Pb collisions at $\sqrt{s_{NN}} = 2.76$ TeV was recently discussed in Ref. [15]. Therefore, the study of pp , p - A , and A - A collisions as functions of charged particle multiplicity has gathered much attention recently, both experimentally and theoretically.

The nonperturbative particle creation mechanisms in strong external fields play important roles from e^+e^- pair creation in quantum electrodynamics (QED) [16] to pair creation of fermions and bosons in strong non-Abelian fields [17–30]. In high-energy heavy-ion collisions, strong color fields are expected to be produced between the partons of the projectile and target. Particle production in high-energy pp and A - A collisions can be described within chromoelectric flux tube (strings) models [31–33].

In a string fragmentation phenomenology, it has been proposed that the observed strong enhancement of strange particle production transverse momentum distribution in nuclear collisions could be naturally explained via strong longitudinal

*mpetro@nipne.ro

Published by the American Physical Society under the terms of the [Creative Commons Attribution 4.0 International](https://creativecommons.org/licenses/by/4.0/) license. Further distribution of this work must maintain attribution to the author(s) and the published article's title, journal citation, and DOI. Funded by SCOAP³.

color field (SLCF) effects [17–20]. Recently, an extension of color glass condensate (CGC) theory has proposed a more detailed dynamical model of color ropes, GLASMA [34–36].

Strong longitudinal fields (flux tubes, effective strings) decay into new ones by quark antiquark ($q\bar{q}$) or diquark–antidiquark ($qq\bar{q}\bar{q}$) pair production before hadronization. Because of the confinement, the color of these strings is restricted to a small area in transverse space [24]. With increasing energy of the colliding particles, the number of strings grows and they start to overlap, producing clusters. This is the origin of the energy density dependence of particle production [37]. The effect of modifying the string tension due to local density has been studied in Monte Carlo models, which are used primarily for heavy-ion collisions [38–43]. In the partons string models (PSM), string fusion and percolation effects on strangeness and heavy flavor production have also been discussed in Refs. [44–47]. A similar model with string fusion into color ropes is considered in the dipole evolution in impact parameter space and rapidity (DIPSY) [11,48,49]. String collective effects were also introduced in a multipomeron exchange model to improve the production of hadrons in pp collisions at the LHC energies [50–52].

Heavy ion jet interacting (HIJING)–type models [32,33], HIJING2.0 [53,54], and HIJING/ $B\bar{B}$ v2.0 [55–65] were developed in order to explain the hadron production in pp , p - A , and A - A collisions. These approaches are based on a two-component geometrical model of minijet production and soft interaction and incorporate nuclear effects such as *shadowing* and *jet quenching*, via final-state jet medium interaction. The HIJING/ $B\bar{B}$ v2.0 model [57,59] includes new dynamical effects associated with long-range coherent fields (i.e., strong longitudinal color fields, SLCF), via baryon junctions and loops [56,66]. At RHIC, it was shown [55–57] that the dynamics of strangeness production deviates from calculations based on Schwinger-like estimates for homogeneous and constant color fields [16], pointing to a possible contribution of fluctuations of transient SLCF. These fields are rather similar to those which could appear in a GLASMA [35] at the initial stage of the collisions. The typical field strength of SLCF at ultrarelativistic energies, in a scenario with QGP phase transition, was estimated to be about 5–12 GeV/fm [67].

Global observables and identified particle (ID) data, including (multi)strange particles production in pp [59,60,63] p -Pb [62,64,65], and Pb-Pb collisions [61] at the LHC energies were successfully described by the HIJING/ $B\bar{B}$ v2.0 model. However, correlations among different measurable quantities in multiparticle production offer a better way to constrain the models. In this paper, we extend our study to identified particles (i.e., π , K , p , Λ , Ξ , Ω , and their antiparticles) produced in small collision systems. We will perform a detailed analysis of correlations between average transverse momentum $\langle p_T \rangle$ and charged particle multiplicity (N_{ch}^*) and of the ratio of double differential cross sections normalized to the charged particle densities ($dN_{\text{ch}}/d\eta$) versus multiplicity, i.e.,

$$R_{\text{mb}}(\text{cen}) = \left(\frac{d^2 N}{dy dp_T} \right)_i^{\text{cen}} / \left(\frac{d^2 N}{dy dp_T} \right)_i^{\text{ppMB}}, \quad (1)$$

where i denotes identified particles in pp collisions and “cen” stands for multiplicity event classes. We will consider high-multiplicity (HM; $N_{\text{ch}} > 100$) and low-multiplicity (LM; $N_{\text{ch}} < 100$) classes. MB stand for minimum-bias events. The charged-particle densities $dN_{\text{ch}}/d\eta$ are integrated values at mid-pseudorapidity $|\eta| < 0.5$ for that class of events. The p_T distributions of ID particles were recently measured in pp collisions at $\sqrt{s} = 7$ TeV for different multiplicity classes of events by the ALICE Collaboration [68–71].

II. HIJING/ $B\bar{B}$ V2.0 MODEL

The HIJING 1.0 model has been discussed in detail in our previous papers [59,60,63]. Here, we briefly summarize the main assumptions and parameters determined as in Ref. [59].

The production rate for a quark pair ($q\bar{q}$) per unit volume for a uniform chromoelectric flux tube with field (E) is

$$\Gamma = \frac{\kappa^2}{4\pi^3} \exp\left(-\frac{\pi m_q^2}{\kappa}\right) \quad (2)$$

[19,72,73], and strong chromoelectric fields are required, $\kappa/m_q^2 > 1$, for a significant production rate. Consequently, the production rate of a heavy quark pair $Q\bar{Q}$ is suppressed by a factor $\gamma_{Q\bar{Q}}$ [72]:

$$\gamma_{Q\bar{Q}} = \frac{\Gamma_{Q\bar{Q}}}{\Gamma_{q\bar{q}}} = \exp\left[-\frac{\pi(m_Q^2 - m_q^2)}{\kappa}\right], \quad (3)$$

The suppression factors are calculated for $Q = qq$ (diquark), $Q = s$ (strange), $Q = c$ (charm), and $Q = b$ (bottom) (q means u or d quark). The quark masses used in the present paper are $m_s = 0.12$ GeV, $m_c = 1.27$ GeV, $m_b = 4.16$ GeV [74], and for diquark $m_{\text{qq}} = 0.45$ GeV [75]. The following effective masses $M_{qq}^{\text{eff}} = 0.5$ GeV, $M_s^{\text{eff}} = 0.28$ GeV, and $M_c^{\text{eff}} = 1.27$ GeV have been considered. For these values and a vacuum string tension $\kappa_0 = 1$ GeV/fm, Eq. (3) gives the following suppression of heavier quark production pairs: $u\bar{u} : d\bar{d} : qq\bar{q}\bar{q} : s\bar{s} : c\bar{c} \approx 1 : 1 : 0.02 : 0.3 : 10^{-11}$ [63]. On the other hand, if the effective string tension value κ increases to $\kappa = f_\kappa \kappa_0$ (with $f_\kappa > 1$), as is the case for a color rope, the value of $\gamma_{Q\bar{Q}}$ increases. A similar increase of $\gamma_{Q\bar{Q}}$ is obtained if the quark mass decreases from m_Q to $m_Q/\sqrt{f_\kappa}$. It was shown [59] that such a dynamical mechanism gives better agreement with the measured strange meson/hyperon ratios at the Tevatron and at LHC energies. It is also known that the A - A collision data are reproduced using flux tubes with much larger string tension relative to the fundamental string tension linking a mesonic quark-antiquark pair [17,24,76]. As the initial energy densities produced in the collision, ϵ_{ini} , are proportional to mean field values $\langle E^2 \rangle$ [24], $\kappa = e_{\text{eff}} E$, and $\epsilon_{\text{ini}} \propto \kappa^2$. Based on the Bjorken approach, ϵ_{ini} is proportional with charged particle density at midrapidity. Therefore, $\kappa^2 \propto (dN_{\text{ch}}/d\eta)_{\eta=0}$ and $\kappa \propto Q_{\text{sat},p}$, similar to the CGC model, as discussed in Ref. [60]. The energy dependence of the charged-particle density at midrapidity in pp collisions up to the LHC energies was described using a power law dependence,

$$\kappa(s) = \kappa_0 (s/s_0)^{0.04} \text{ GeV/fm}, \quad (4)$$

consistent with the value deduced in the CGC model for $Q_{\text{sat},p}$ [77].

Following Eq. (4), at $\sqrt{s} = 0.2$ TeV the effective string tension value is $\kappa = 1.5$ GeV/fm while at $\sqrt{s} = 7$ TeV $\kappa = 2.0$ GeV/fm. Previous papers [56–59,61,63] presented the dependence of different observables on the string tension values. The phenomenological parametrization, Eq. (4), is supported by the experimental results on charged-particle densities at midrapidity $(dN_{\text{ch}}/d\eta)_{\eta=0}$. Within the error bars, the $\sqrt{(dN_{\text{ch}}/d\eta)_{\eta=0}}$ shows a power law $s^{0.05}$ dependence for inelastic pp and $s^{0.055}$ dependence for nonsingle diffractive events [78,79]. In A - A collisions, the effective string tension value could also increase because of in-medium effects [61] or as a function of centrality. This increase is considered in our phenomenology by an analogy with the CGC model, i.e., $\kappa(s, A) \propto Q_{\text{sat},A}(s, A) \propto Q_{\text{sat},p}(s)A^{1/6}$. Therefore, in the present analysis for A - A collisions, we used $\kappa = \kappa(s, A)$:

$$\kappa(s, A)_{\text{LHC}} = \kappa(s)A^{0.167} = \kappa_0 (s/s_0)^{0.04} A^{0.167} \text{ GeV/fm.} \quad (5)$$

Equation (5) gives $\kappa(s, A)_{\text{LHC}} \approx 5$ GeV/fm, for Pb-Pb collisions at $\sqrt{s_{NN}} = 2.76$ TeV. The suppression factor $\gamma_{Q\bar{Q}}$ approaches unity in Pb-Pb collisions at $\sqrt{s_{NN}} = 2.76$ TeV for $\kappa \geq 5$ GeV/fm. The mean effective values of the string tension $\kappa(s)$ for pp collisions [Eq. (4)] and $\kappa(s, A)$ for Pb-Pb collisions [Eq. (5)] are used in the present calculations. As a consequence, the various suppression factors and the intrinsic (primordial) transverse momentum k_T increase [59,60]. We would like to mention also that for a better description of the baryon-meson anomaly evidenced at RHIC and LHC energies, we introduced specific $J\bar{J}$ loops (for details, see Refs. [61,63]). The absolute yield of charged particles, $dN_{\text{ch}}/d\eta$, is sensitive to the low $p_T < 2$ GeV/ c nonperturbative hadronization dynamics. This was considered based on string JETSET fragmentation [80,81] constrained by lower energy ee , ep , pp data. The hard pQCD contribution is estimated in HIJING/ $B\bar{B}$ v2.0 using PYTHIA [82] subroutines. Details on shadowing and jet quenching are given in Ref. [60]. The main advantage of HIJING/ $B\bar{B}$ v2.0 over PYTHIA 6.4 resides in the SLCF color rope effects that arise from longitudinal fields amplified by the random walk in color space of the high- x valence partons in A - A collisions. A broad fluctuation spectrum of the effective string tension could be induced by this random walk. The present work is focused on the effect of a larger effective value $\kappa > 1$ GeV/fm on the production of identified particles measured in Pb-Pb, p -Pb, and pp collisions at LHC energies. While the present approach is based on the time-independent strength of color field, in reality the production of $Q\bar{Q}$ pairs is a far-from-equilibrium, time- and space-dependent, complex phenomenon. Therefore, the influence of time-dependent fluctuations cannot be addressed within the present approach.

III. NUMERICAL RESULTS AND DISCUSSION

A. The average transverse momentum $\langle p_T \rangle$ versus N_{ch} correlations

The HIJING/ $B\bar{B}$ v2.0 model predicts many experimental observables (charged hadron pseudorapidity distributions,

transverse momentum spectra, identified particle spectra, baryon-to-meson ratios) using the above values for the effective string tension, κ (see Sec. II) [59,60,62–64].

The ALICE Collaboration has reported measurements of the average transverse momentum $\langle p_T \rangle$ versus charged particles N_{ch}^* at central rapidity in pp at $\sqrt{s} = 7$ TeV, p -Pb at $\sqrt{s_{NN}} = 5.02$ TeV, and Pb-Pb collisions at $\sqrt{s_{NN}} = 2.76$ TeV [83]. The analysis range was restricted to a transverse momentum $0.15 < p_T < 10$ GeV/ c and to a mid-pseudorapidity range $|\eta| < 0.3$. Figure 1 shows the results obtained with the HIJING/ $B\bar{B}$ v2.0 model (open symbols) for pp collisions at $\sqrt{s} = 7$ TeV (left panel) and p -Pb at $\sqrt{s_{NN}} = 5.02$ TeV (right panel). As we can see in Fig. 1, a continuous increase of $\langle p_T \rangle$ with N_{ch}^* is observed for both reactions. Therefore, to calculate the correlation $\langle p_T \rangle_{N_{\text{ch}}}$ versus N_{ch}^* , we first investigate in a model of hadronizing strings if the above increase could be attributed to the effects of SLCF and the results are given for different strengths of color fields quantified by an effective value of the string tension from $\kappa = 1$ GeV/fm (default value) up to $\kappa = 5$ GeV/fm. As we could remark, the calculations with the default value $\kappa = 1$ GeV/fm describe better the pp data. An alternative explanation of the increase of $\langle p_T \rangle$ with N_{ch}^* should be naturally given in the context of the fragmentation of multiple minijets embedded in HIJING-type models [32] and was discussed in the early 1990s for $p\bar{p}$ collisions at $\sqrt{s} = 1.8$ TeV [18,20,33]. The large-multiplicity events are dominated by multiple minijets while low-multiplicity events are dominated by no jet production. Few partons are enough to explain the increase of $\langle p_T \rangle$ with N_{ch}^* . We may also conclude that these correlations in pp collisions at $\sqrt{s} = 7$ TeV are not sensitive to the soft fragmentation region, where we expect that SLCF effects are dominant. In contrast, for p -Pb collisions, the theoretical calculations compared to data [83] in Fig. 1 (right panel) show better agreement if the value of κ is increased from $\kappa = 1$ to $\kappa = 3$ GeV/fm. We will study now the effect of an enhanced value of the effective string tension κ on the correlation of $\langle p_T \rangle$ versus N_{ch}^* for ID particle in pp and p -Pb collisions at $\sqrt{s} = 7$ TeV, and $\sqrt{s_{NN}} = 5.02$ TeV, respectively. Shown in Fig. 2 are our theoretical calculations (open symbols) in comparison with data [68,69,71] on the $\langle p_T \rangle$ of $\pi^+ + \pi^-$, $K^+ + K^-$, $p + \bar{p}$, $\Xi^- + \bar{\Xi}^+$, and $\Omega^- + \bar{\Omega}^+$ for $0 < p_T < 10$ GeV/ c and midrapidity $|y| < 0.5$ versus charged particle multiplicity N_{ch}^* (selected in the $|\eta| < 0.5$ range) for pp collisions at $\sqrt{s} = 7$ TeV. The results (open symbols) are given for two values of the effective string tension $\kappa = 2$ GeV/fm (left panel) and $\kappa = 5$ GeV/fm (right panel). The data show an increase of $\langle p_T \rangle$ with increased multiplicity and with the particle mass, facts fairly well described by the model. Note that for clarity we did not include here the results for $\Lambda + \bar{\Lambda}$. Since the mass difference between Λ and proton is very small, the results are almost the same [68].

The $\langle p_T \rangle$ increases with increasing multiplicity as the effect of the strong longitudinal color field embedded in our model. A modified string fragmentation using $\kappa = 2$ GeV/fm increase the production rate for heavier particles. Moreover, an increase of the width of the primordial (intrinsic) transverse momentum (k_T) distribution from the default value of the Gaussian ($\sigma_q = \sigma_{\text{qq}} = 0.350$ GeV/ c) to larger

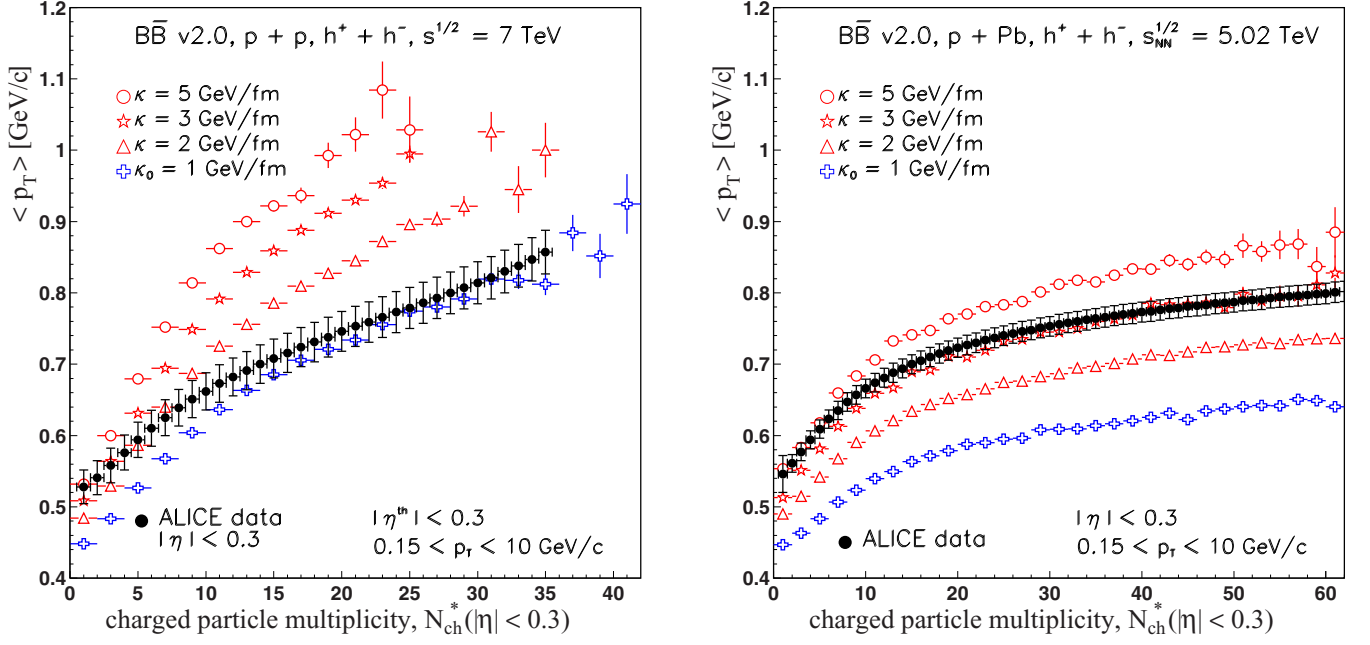


FIG. 1. Open symbols: HIJING/ $B\bar{B}$ v2.0 predictions for the average transverse momentum ($\langle p_T \rangle$) of charged particles as a function of multiplicity at mid-pseudorapidity N_{ch}^* . Left panel: pp collisions at $\sqrt{s} = 7$ TeV for $0.15 < p_T < 10$ GeV/c and mid-pseudorapidity $|\eta| < 0.3$. Right panel: p -Pb collisions at $\sqrt{s_{NN}} = 5.02$ TeV for $0.15 < p_T < 10$ GeV/c and midrapidity $|\eta| < 0.3$. The theoretical results are obtained for different effective string tensions increasing from $\kappa = 1$ GeV/fm (default) up to $\kappa = 5$ GeV/fm. The ALICE data (filled circles) are from Ref. [83]. The errors represent systematic uncertainties on $\langle p_T \rangle$. The statistical errors are negligible.

values for the (anti)quark ($\sigma_q'' = \sqrt{\kappa/\kappa_0}\sigma_q$) and (anti)diquark ($\sigma_{qq}'' = \sqrt{\kappa/\kappa_0}f\sigma_{qq}$), where $f = 3$ [59,60], contribute also to an increase of the heavier particle production rate. This

provides consistent evidence that modified fragmentation obtained by an enhanced κ from the default value $\kappa = 1$ GeV/fm and minijet production as implemented in the

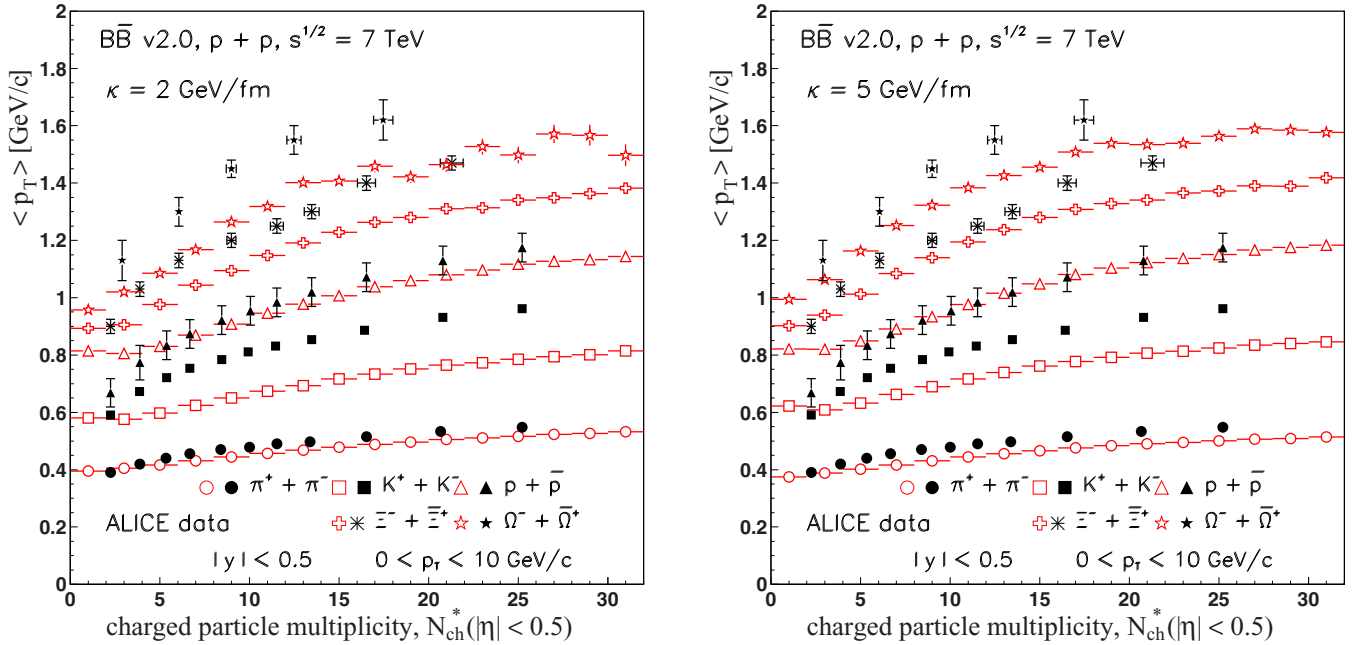


FIG. 2. Open symbols: HIJING/ $B\bar{B}$ v2.0 predictions for the average transverse momentum ($\langle p_T \rangle$) of identified particle for $0 < p_T < 10$ GeV/c and midrapidity $|y| < 0.5$ as function of charged particle multiplicity, N_{ch}^* in pp collisions at $\sqrt{s} = 7$ TeV. The results are obtained with an effective string tension value, $\kappa = 2$ GeV/fm (left side) and $\kappa = 5$ GeV/fm (right side). For clarity, we do not include the results for Λ . The ALICE preliminary data (filled symbols) are from Refs. [68,69,71]. Only statistical error bars are shown.

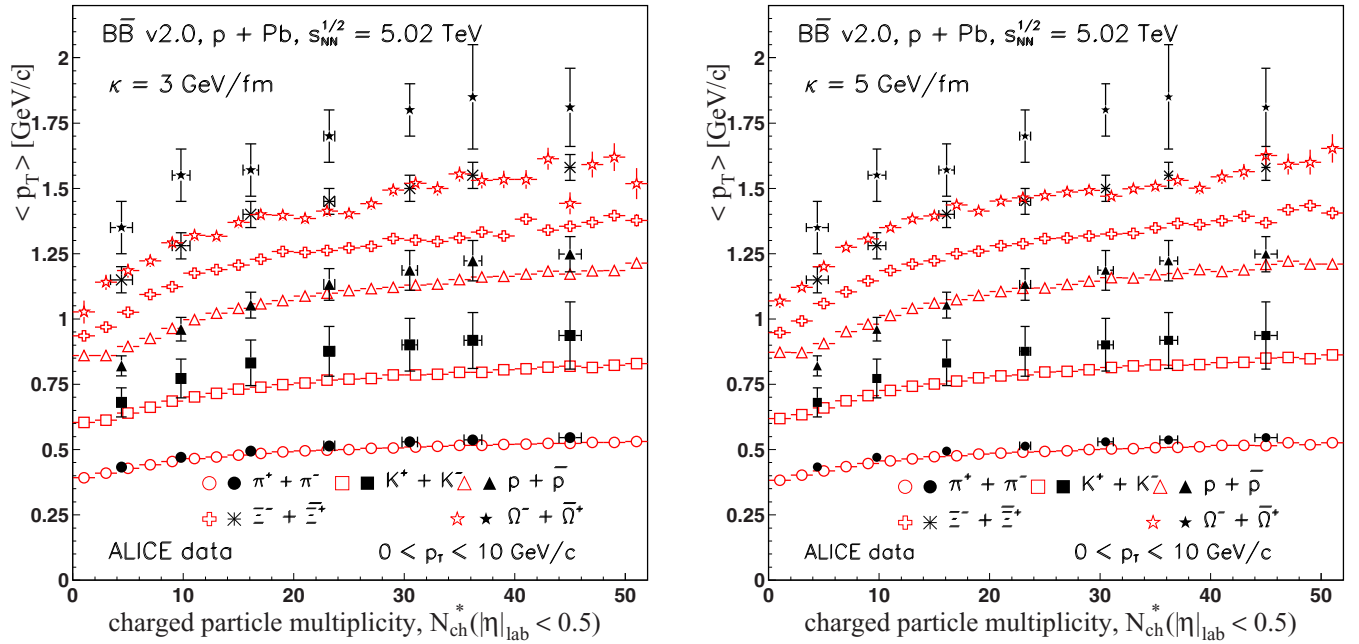


FIG. 3. Open symbols: HIJING/ $B\bar{B}$ v2.0 predictions for the average transverse momentum ($\langle p_T \rangle$) of identified particle in the range $0 < p_T < 10$ GeV/c and midrapidity $0.0 < y_{cm} < 0.5$ as function of charged particle multiplicity, N_{ch}^* in p -Pb collisions at $\sqrt{s_{NN}} = 5.02$ TeV. The results (open symbols) are obtained with an effective string tension value, $\kappa = 3$ GeV/fm (left side) and $\kappa = 5$ GeV/fm (right side). For clarity, we do not include the results for Λ . The ALICE data (filled symbols) are from Ref. [88]. Only statistical error bars are shown.

HIJING/ $B\bar{B}$ v2.0 model lead to a fairly good description of these observables. However, the model gives only partial agreement with $\langle p_T \rangle$ values for ID particle at high multiplicity. The model describes well the $\langle p_T \rangle$ of $\pi^+ + \pi^-$, $p + \bar{p}$, and $\Lambda + \bar{\Lambda}$, but the results strongly underestimate the $\langle p_T \rangle$ of (multi)strange particles as $K^+ + K^-$, $\Xi^- + \bar{\Xi}^+$, and $\Omega^- + \bar{\Omega}^+$. We studied if one can find a scenario that would give a larger enhancement of the $\langle p_T \rangle$ of (multi)strange particles. We consider the effect of a further increase of the string tension to $\kappa = 5$ GeV/fm and the results are presented in Fig. 2 (right panel). Note that a value $\kappa \approx 5\kappa_0$ GeV/fm is also supported by the calculations at finite temperature (T) of potentials associated with a $q\bar{q}$ pair separated by a distance r [84]. The finite-temperature (T) form of the $q\bar{q}$ potential has been calculated by means of lattice QCD [85]. At finite temperature, there are two potentials associated with a $q\bar{q}$ pair separated by a distance r : the free energy $F(T, r)$ and potential energy $V(T, r)$. The free and potential energies actually correspond to slow and fast (relative) motion of the charges, respectively. Infrared-sensitive variables such as string tension and their derivatives with respect to r are very helpful to identify specific degrees of freedom of the plasma. Since the confinement of color in non-Abelian theories is due to the magnetic degree of freedom, the magnetic component is expected to be present in the plasma as well. In the presence of the *chromomagnetic scenario*, it was shown that the effective string tension of the free energy $\kappa = \kappa_F$ decreases with T to near zero at critical temperature (T_c). In contrast, the effective string tension of the potential energy (corresponding to a fast relative motion of the charges) $\kappa = \kappa_V$ remains nonzero below $\sim T = 1.3 T_c$ with a peak value at

T_c of about 5 times the vacuum tension κ_0 ($\kappa_V = 5$ GeV/fm) [84,86]. The above calculations for $\kappa \approx 5\kappa_0$ GeV/fm result in only a modest increase of the $\langle p_T \rangle$ of kaons ($K^+ + K^-$) by 10–15% and a better description of $\langle p_T \rangle$ of multistrange particles ($\Xi^- + \bar{\Xi}^+$ and $\Omega^- + \bar{\Omega}^+$) only at low multiplicity ($N_{ch} < 15$). In our calculations, the discrepancy obtained for $\langle p_T \rangle$ of kaons does not appear to turn over for $\kappa = 5$ GeV/fm as expected. This discrepancy may be related to the kaon enhancement reported first in Ref. [87] at Tevatron energies and confirmed now at LHC energies [68,69,71]. Note that new PYTHIA8 model, which includes a specific increase of the string tension values [10], also could not describe better the $\langle p_T \rangle$ of kaons in pp collisions at $\sqrt{s} = 7$ TeV. Further analysis is necessary in order to draw a definite conclusion. In the HIJING/ $B\bar{B}$ v2.0 model, the collective behavior is a consequence of the confining strong color fields, resulting in an interaction between strings that is without diffusion or loss of energy [11]. Therefore, for values of string tension between 5 and 10 GeV/fm (the calculations are not included here), saturation seems to set in, possibly as an effect of energy and momentum conservation as well as saturation of strangeness suppression factors. Similar conclusions could be drawn for $\langle p_T \rangle$ of ID particles versus charged-particle multiplicity, N_{ch}^* measured in p -Pb collisions at $\sqrt{s_{NN}} = 5.02$ TeV. The results (open symbols) are obtained in the range $0 < p_T < 10$ GeV/c and midrapidity $0.0 < y_{cm} < 0.5$, and are shown in Fig. 3. Up to now, the microscopic origin of enhanced (multi)strange particles production is not known. It is, therefore, a valid question whether small systems (high-multiplicity pp and p -Pb) exhibit any behavior of the kind observed in heavy-ion collisions. Bjorken suggested the possibility of deconfinement

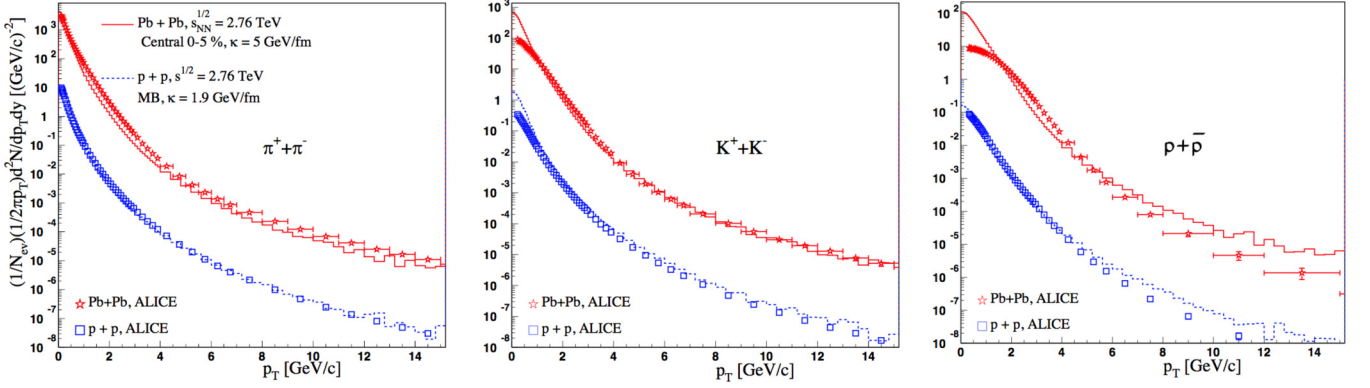


FIG. 4. HIJING/ $B\bar{B}$ v2.0 predictions for the invariant yields of identified particles in central Pb-Pb collisions (solid histograms) and pp collisions (dashed histograms) at c.m. energy 2.76 TeV. The results are obtained using $\kappa = 5$ GeV/fm ($\kappa = 1.9$ GeV/fm) for Pb-Pb (pp), respectively. The ALICE data are from Ref. [92]. The error include systematic uncertainties.

in pp collisions [89]. Van Hove [90] and Campanini [91] suggested that an anomalous behavior of average transverse momentum ($\langle p_T \rangle$) as a function of multiplicity could be a signal for the occurrence of a phase transition in hadronic matter, i.e., formation of a *mini quark-gluon plasma* (mQGP). The

long-range near-side ridge in particle correlations observed in high-multiplicity events [1–4], collective flow [5–7], and strangeness enhancement [8] were evidenced in pp collisions at the LHC energies and support such a hypothesis. However, a fundamental question remains: Are such correlations of

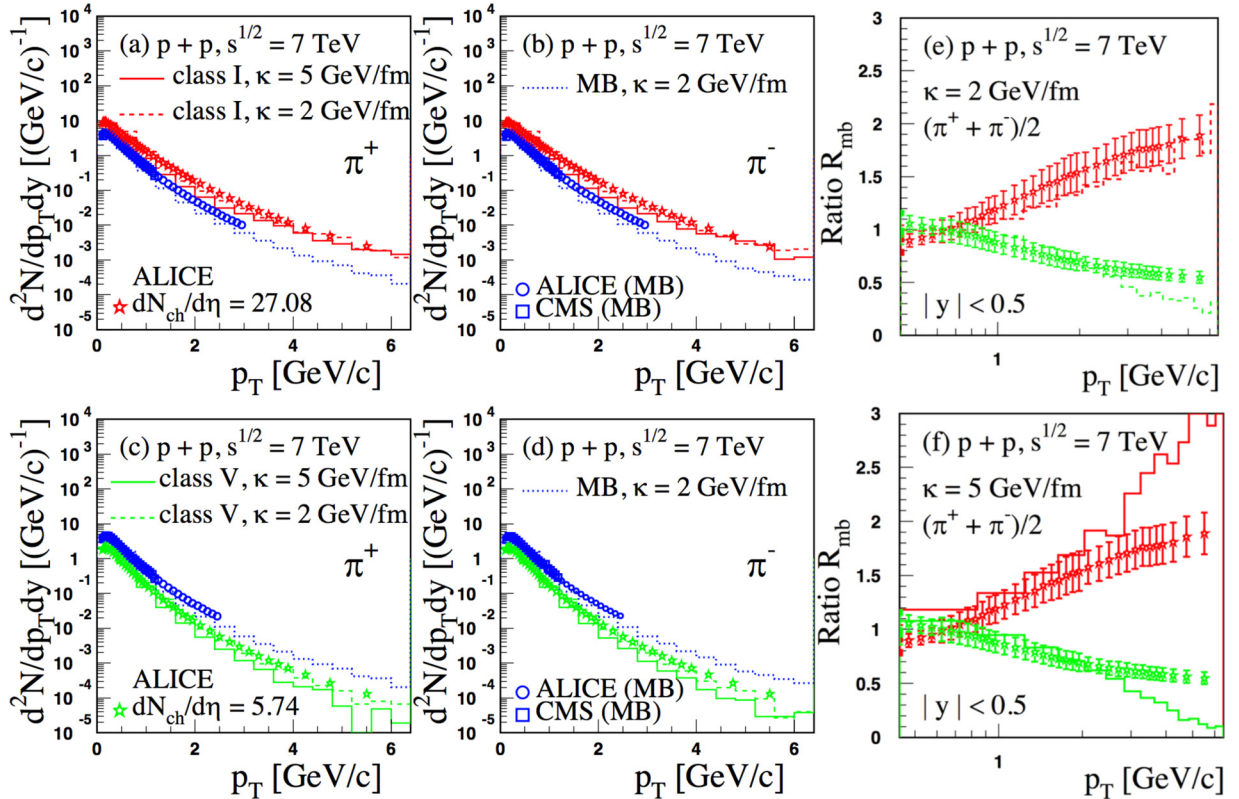


FIG. 5. HIJING/ $B\bar{B}$ v2.0 results for transverse momentum (p_T) distributions at midrapidity for charged pions in two multiplicity classes (see text for explanation). The results for high- (low-) multiplicity classes of events are presented in the panels (a) and (b) and panels (c) and (d), respectively. The solid (dashed) histograms are obtained using $\kappa = 5$ GeV/fm ($\kappa = 2$ GeV/fm) for high (class I) and low (class V) multiplicity classes of events. The results for minimum-bias pp collisions obtained for $\kappa = 2$ GeV/fm (dotted histograms) are included and compared to data from ALICE [93] (open circles) and CMS Collaborations [94] (open squares). Panels (e) and (f) include the ratios R_{mb} obtained using $\kappa = 2$ GeV/fm and $\kappa = 5$ GeV/fm, respectively. The upper dashed and solid histograms are for HM (class I), and the lower dashed and solid histograms are for LM (class V) class of events. The experimental ratio R_{mb} was calculated by us based on average p_T spectra of particles and antiparticles measured (open stars) by the ALICE Collaboration [69–71]. Only statistical error bars are shown.

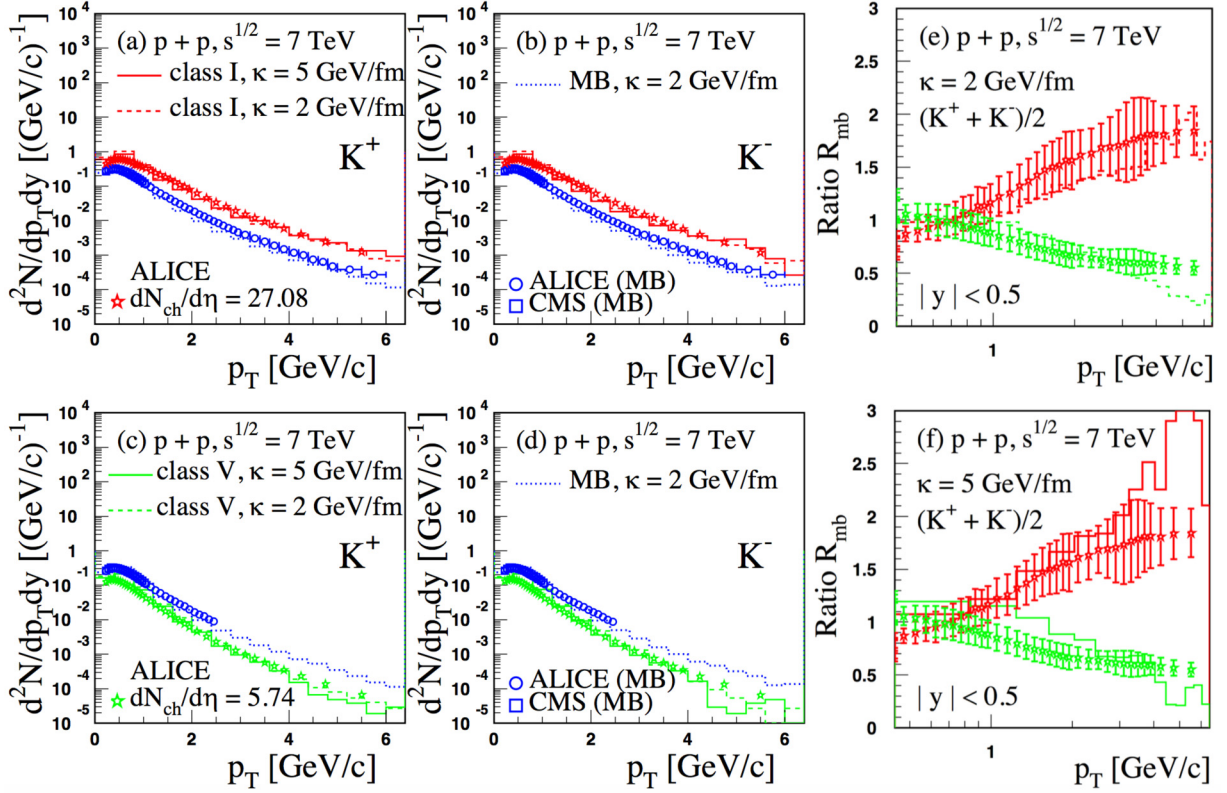


FIG. 6. The same as in Fig. 5 for charged kaons.

(p_T) versus N_{ch}^* for ID particles in small systems (pp , p -Pb collisions) of collective origin, attributed to a hydrodynamic evolution like in Pb-Pb collisions, or are they a natural consequence due to initial-state dynamics that show up in the final-state observables [11]? Collective hydrodynamic flow as a signature of sQGP is well established in Pb-Pb collisions at LHC energies. Such conclusions can be drawn from measurements of the invariant transverse momentum spectra of identified particles in central Pb-Pb collisions at $\sqrt{s_{NN}} = 2.76$ TeV. In Fig. 4, we consider the results for light identified charged hadrons in Pb-Pb collisions (solid histograms) in comparison with those produced in pp collisions (dashed histograms) at $\sqrt{s} = 2.76$ TeV. The experimental data are from the ALICE Collaboration [92]. The calculations are performed taking an effective value of the string tension κ with an energy and mass dependence as in Eq. (5), i.e., $\kappa(s, A)_{\text{LHC}} = \kappa(s)A^{0.167} = \kappa_0 (s/s_0)^{0.04} A^{0.167}$ GeV/fm. This formula leads to $\kappa(s, A)_{\text{LHC}} \approx 5$ GeV/fm, in Pb-Pb collisions at c.m. energy per nucleon $\sqrt{s_{NN}} = 2.76$ TeV. In pp collisions, we consider only variation with energy, i.e., $\kappa(s) = \kappa_0 (s/s_0)^{0.04}$ GeV/fm, which gives a value of $\kappa \approx 1.9$ GeV/fm. The results obtained within our model show a partial agreement with data, since a large pressure in the initial state, leading to flow especially for (anti)protons, is not considered in string fragmentation models.

B. Ratio of normalized transverse momentum distributions

The measured transverse momentum distributions for ID particles for different multiplicity bins have been recently

reported by the ALICE Collaboration in pp collisions at $\sqrt{s} = 7$ TeV [68–71]. The transverse momentum spectra of the identified hadrons (ID) were measured for several event multiplicity classes from the highest (class I) to the lowest (class X) multiplicity class, corresponding to approximately 3.5 and 0.4 times the average value in the integrated sample ($\langle dN_{\text{ch}}/d\eta \rangle^{\text{MB}} \approx 6.0$), respectively. In the experiment, the multiplicity classes are defined based on the total charge deposited in the V0A and V0C detectors located at forward ($2.8 < \eta < 5.1$) and backward ($-3.7 < \eta < -1.7$) pseudorapidity regions, respectively. The event multiplicity estimator is taken to be the sum of V0A and V0C signals denoted as VOM. The average charged-particle density ($\langle dN_{\text{ch}}^{\text{exp}}/d\eta \rangle$), is estimated within each such multiplicity class by the average of the track distributions in the region $|\eta| < 0.5$. Based on these spectra and minimum-bias results, we will study here the ratio of double differential cross sections normalized to the charged-particle densities $dN_{\text{ch}}^{\text{th}}/d\eta$ versus multiplicity, i.e., the ratio R_{mb} defined in Eq. (1). For theoretical calculations within the HIJING/ $B\bar{B}$ v2.0 model, we will chose different classes of event activity cutting on the total multiplicity (N_{ch}) for each 10^6 set of events generated using two effective string tension values, i.e., $\kappa = 2.0$ GeV/fm and an enhanced value of $\kappa = 5.0$ GeV/fm. Moreover, the average charged-particle density is estimated (for both set of events) within each multiplicity class of events, by the integrated value of $dN_{\text{ch}}^{\text{th}}/d\eta$ at mid-pseudorapidity ($|\eta| < 0.5$). In addition, we generate also 10^6 minimum-bias (MB) events for $\kappa = 2.0$ GeV/fm. Note that for this selection theoretical calculations give an integrated charged particle density at mid-pseudorapidity

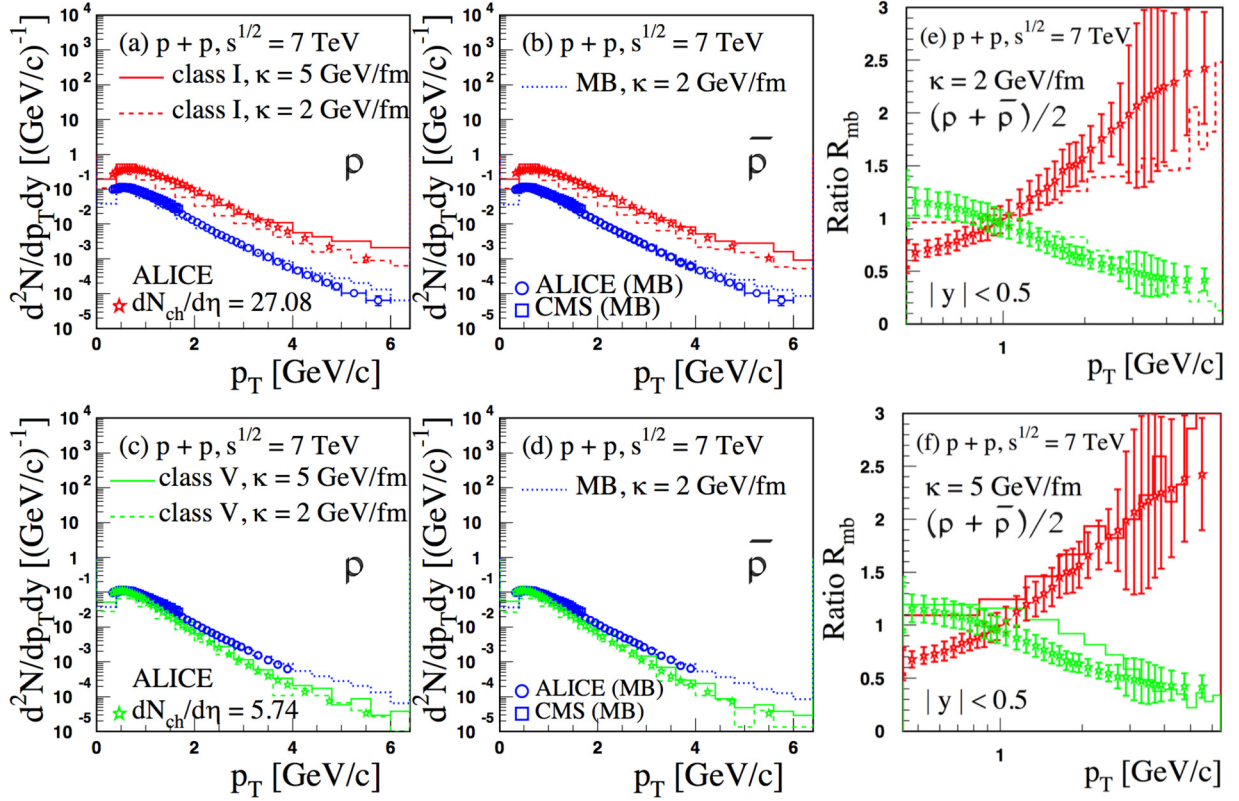


FIG. 7. The same as in Fig. 5 for protons and antiprotons.

($|\eta| < 0.5$), $(dN_{\text{ch}}^{\text{th}}/d\eta)^{\text{MB}} = 5.7$, close to the experimental value $(dN_{\text{ch}}/d\eta)^{\text{MB}} \approx 6.0$ quoted above.

We will consider six classes of event activity, defined as follows:

- (1) class I: $200 \leq N_{\text{ch}} < 300$; $dN_{\text{ch}}^{\text{th}}/d\eta = 30.9$ (for $\kappa = 2$ GeV/fm); $dN_{\text{ch}}^{\text{th}}/d\eta = 25.2$ (for $\kappa = 5$ GeV/fm).
- (2) class II: $120 \leq N_{\text{ch}} < 200$; $dN_{\text{ch}}^{\text{th}}/d\eta = 18.6$ (for $\kappa = 2$ GeV/fm); $dN_{\text{ch}}^{\text{th}}/d\eta = 15.1$ (for $\kappa = 5$ GeV/fm).
- (3) class III: $100 \leq N_{\text{ch}} < 120$; $dN_{\text{ch}}^{\text{th}}/d\eta = 12.5$ (for $\kappa = 2$ GeV/fm); $dN_{\text{ch}}^{\text{th}}/d\eta = 10.3$ (for $\kappa = 5$ GeV/fm).
- (4) class IV: $80 \leq N_{\text{ch}} < 100$; $dN_{\text{ch}}^{\text{th}}/d\eta = 9.7$ (for $\kappa = 2$ GeV/fm); $dN_{\text{ch}}^{\text{th}}/d\eta = 7.8$ (for $\kappa = 5$ GeV/fm).
- (5) class V: $60 \leq N_{\text{ch}} < 80$; $dN_{\text{ch}}^{\text{th}}/d\eta = 7.1$ (for $\kappa = 2$ GeV/fm); $dN_{\text{ch}}^{\text{th}}/d\eta = 5.7$ (for $\kappa = 5$ GeV/fm).
- (6) class VI: $30 \leq N_{\text{ch}} < 60$; $dN_{\text{ch}}^{\text{th}}/d\eta = 4.7$ (for $\kappa = 2$ GeV/fm); $dN_{\text{ch}}^{\text{th}}/d\eta = 3.9$ (for $\kappa = 5$ GeV/fm).

For comparison to data from Refs. [69,70], we show in Figs. 5, 6, and 7 the results of the HIJING/ $B\bar{B}$ v2.0 predictions for transverse momentum distributions at midrapidity for light hadrons, i.e., π , K , p and their antiparticles in two multiplicity classes, class I [Figs. 5–7(a) and 5–7(b)] and class V [Figs. 5–7(c) and 5–7(d)]. The model estimates are represented by solid (dashed) histograms for $\kappa = 5$ GeV/fm and $\kappa = 2$ GeV/fm, respectively. For comparison with data, the experimental spectra (open stars) are chosen for an average value of $\langle dN_{\text{ch}}^{\text{exp}}/d\eta \rangle$ similar with those obtained in the model, $dN_{\text{ch}}^{\text{th}}/d\eta$ (see the above six classes of event activity). The

results for minimum bias pp collisions obtained for $\kappa = 2$ GeV/fm are represented by dotted histograms. Data for MB are from Ref. [93] (open circles) and Ref. [94] (open squares).

The ratio of double differential cross sections normalized to the charged-particle densities, R_{mb} (calculated by us) is plotted for high (class I) and low (class V) multiplicity classes in Figs. 5–7(e) and 5–7(f) by dashed and solid histograms for $\kappa = 2$ and $\kappa = 5$ GeV/fm, respectively. This ratio is based on average p_T spectra of particles and antiparticles measured (open stars) by the ALICE Collaboration [69–71]. In the calculations, we take into account the variation of strong color (electric) field with energy. The assumed effective value of the string tension is $\kappa = 2$ GeV/fm [Figs. 5–7(e)] corresponding to $\kappa(s) = \kappa_0 (s/s_0)^{0.04}$ GeV/fm [see Eq. (4)]. Since we expect in high-multiplicity proton-proton collisions features that are similar to those observed in Pb-Pb collisions, we consider also the results obtained for an enhanced value of effective string tension to $\kappa = 5$ GeV/fm [see Figs. 5–7(f)]. The agreement with the data is fairly good in the limit of the error bars, except for very low $p_T < 1$ GeV values. The experimental spectra show a small depletion at high multiplicity at very low p_T , indicating possible influence of the radial flow. The transverse momentum spectra of identified particles carrying light quarks and their azimuthal distributions are well described by hydrodynamical models [12,13] at very low p_T . However, as far as in the string model the pressure is not considered, it is not expected to describe such effects which could originate from collective expansion. At low and intermediate

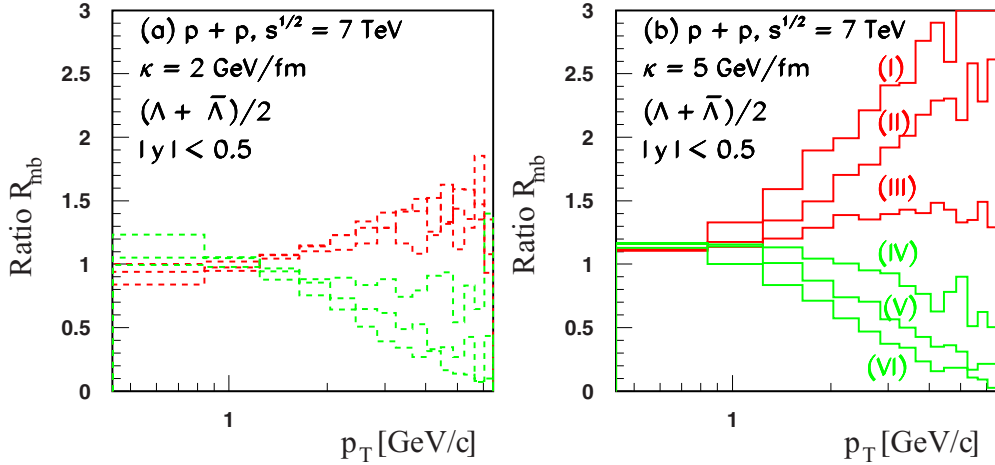


FIG. 8. The HIJING/ $B\bar{B}$ v2.0 model predictions for $\Lambda + \bar{\Lambda}$ produced in pp collisions at $\sqrt{s} = 7$ TeV. The ratios of the normalized p_T distributions, R_{mb} [see Eq. (1)] for six multiplicity classes (see text for explanation) based on average p_T spectra of particle and antiparticle. From top to bottom, the calculations correspond to class I to class VI multiplicity events. Left: The results obtained with $\kappa = 2$ GeV/fm. Right: The results obtained with ($\kappa = 5$ GeV/fm).

p_T ($1 \text{ GeV}/c < p_T < 6 \text{ GeV}/c$), the nonperturbative production mechanism via SLCF produces a clear split between high- and low-multiplicity events. For the highest multiplicity (class I), we see a hardening of the p_T spectra for π , K , p , and their antiparticles. However, within the experimental errors, the agreement between the model predictions

and experiment in terms of R_{mb} is rather similar for both values of the string tension, i.e., $\kappa = 2$ and $\kappa = 5$ GeV/fm for pions and kaons. For protons, the agreement is definitely better at low charged-particle multiplicity (class V) for $\kappa = 2$ GeV/fm and at higher charged-particle multiplicity (class I) for $\kappa = 5$ GeV/fm. Because of strange quark content

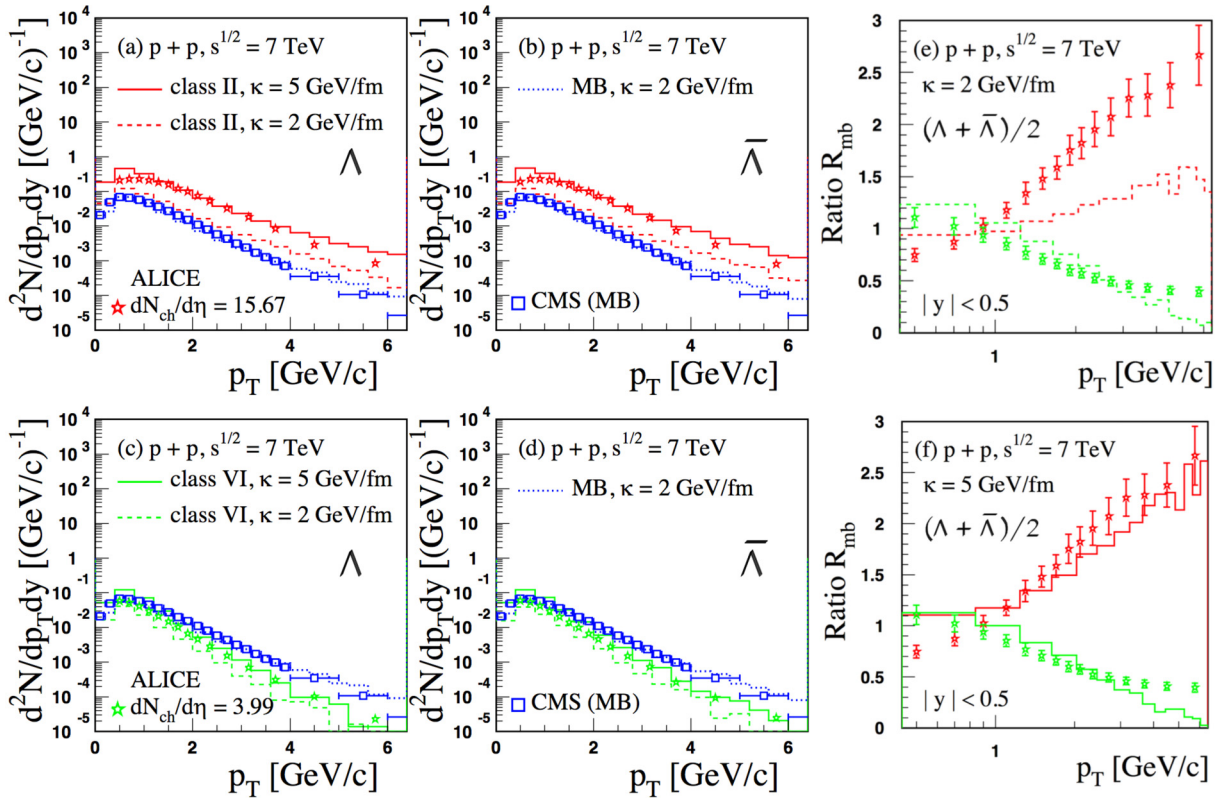


FIG. 9. The same as in Fig. 5 for events of high (class II) and low (class VI) multiplicities. The calculations are for Λ and $\bar{\Lambda}$. The results for minimum-bias pp collisions obtained with $\kappa = 2$ GeV/fm (dotted histograms) are included and compared to data from the CMS Collaboration [94] (open squares). Only statistical error bars are shown.

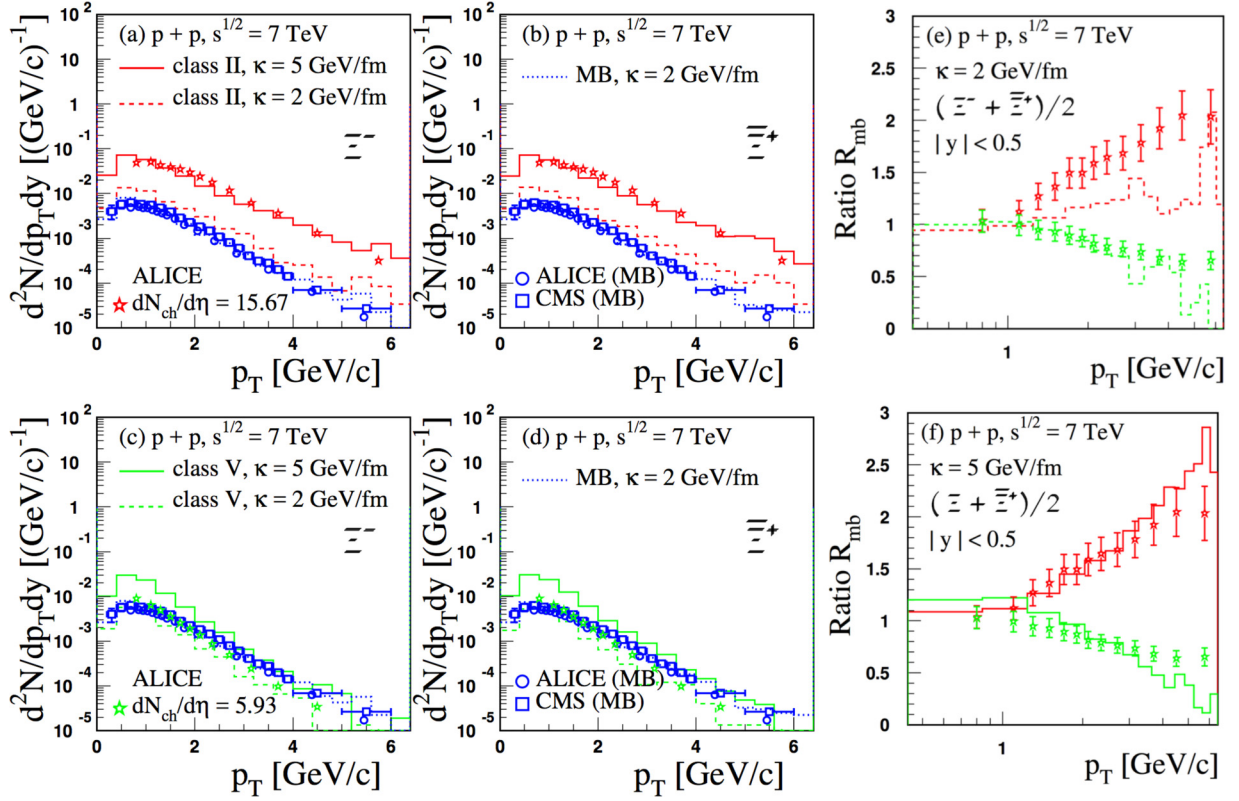


FIG. 10. The same as Fig. 5 for events of high (class II) and low (class V) multiplicities. The calculations are for Ξ^- and $\bar{\Xi}^+$. The results for minimum-bias pp collisions obtained with $\kappa = 2$ GeV/fm (dotted histograms) are included and compared to data from the ALICE [68,69,71] (open circles) and CMS Collaborations [94] (open squares). Only statistical error bars are shown.

of (multi)strange particles, the study of the ratio R_{mb} is of particular interest. Since we expect higher sensitivity to SLCF effects for (multi)strange than for bulk particles, measurements of p_T distributions at midrapidity as well as the ratio R_{mb} could help to confirm these effects, within the phenomenology embedded in the HIJING/ $B\bar{B}$ v2.0 model. Figure 8 show the ratios of the normalized p_T distributions, R_{mb} of $\Lambda + \bar{\Lambda}$ produced in $p+p$ collisions at $\sqrt{s} = 7$ TeV. The results for six multiplicity classes (class I to class VI) based on average p_T spectra of particles and antiparticles are included. From top to bottom, the calculations correspond to highest (class I) to lowest (class VI) multiplicity events. Left (right) panels are the results obtained with $\kappa = 2$ GeV/fm ($\kappa = 5$ GeV/fm), respectively. We remark a clear hardening of the p_T spectra for high multiplicity, especially for $N_{ch} > 100$ (class III to class I events), where a change in the slope is obvious. The effect is more evident for an enhanced effective value of string tension $\kappa = 5$ GeV/fm (see Fig. 8 right panel). Similar results (not included here) are obtained for multistrange particles, i.e., Ξ and Ω . High-multiplicity events have a higher fraction of heavier particles, meaning with a higher strangeness content. We can explain this fact as an effect of strong color field embedded in our model. Note that $N_{ch} > 120$ is also the charged-particle multiplicity above which was observed the enhancement in the near-side long-range two-particle correlation reported by the CMS Collaboration [1]. However, there is no mechanism that produces a ridge in our model.

The experimental fact that pp collisions manifest features similar to those of Pb-Pb collisions [1–8,95] point out the necessity of modifying κ when describing observables in pp collisions for the HM class of events. The calculations with SLCF contributions assume an effective string tension value $\kappa = 2$ GeV/fm, obtained from an energy dependence κ (see Sec. II), while the results with $\kappa = 5$ GeV/fm are obtained based on the above experimental result. Note that a specific size-dependent $\kappa = \kappa(r)$ was considered recently in the PYTHIA 8 model, with r as a new parameter fixed to fit data [10].

Therefore, in Fig. 9 (Λ and $\bar{\Lambda}$), Fig. 10 (Ξ^- and $\bar{\Xi}^+$), and Fig. 11 (Ω^- and $\bar{\Omega}^+$), we show the results obtained for p_T distributions at midrapidity for (multi)strange particles in two event classes, corresponding to high (HM) and low (LM) charged-particle multiplicities. The calculations for minimum-bias events are included and compared to data from Refs. [68,69,94]. As in the previous calculations, comparison to data for HM and LM events is made for p_T spectra obtained for a class of events which give a value of $dN_{ch}^{th}/d\eta$ similar with those obtained in the experiment ($dN_{ch}^{exp}/d\eta$). Theoretical predictions for the p_T dependence of R_{mb} for $\Lambda + \bar{\Lambda}$, $\Xi^- + \bar{\Xi}^+$, and $\Omega^- + \bar{\Omega}^+$ are presented for two scenarios: using $\kappa = 2$ GeV/fm [Figs. 9–11(e)] and an increased value to $\kappa = 5$ GeV/fm [Figs. 9–11(f)]. The results show a clear hardening of p_T spectra in the case of the HM class of events. Moreover, in the case of the LM class of events, the R_{mb} ratio of (multi)strange particles are better described

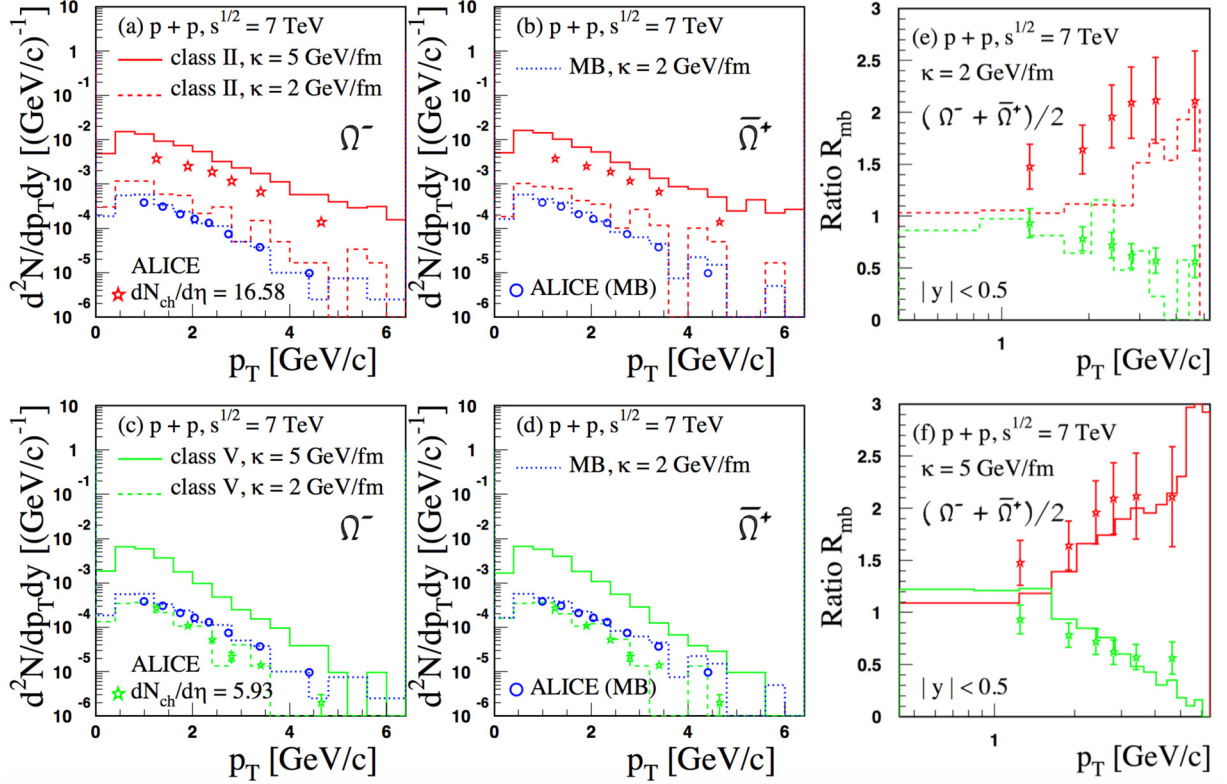


FIG. 11. The same as in Fig. 5 for events of high (class II) and low (class V) multiplicities. The calculations are for Ω^- and $\bar{\Omega}^+$. The results for minimum-bias pp collisions obtained with $\kappa = 2$ GeV/fm (dotted histograms) are included and compared to data (open circles) from the ALICE Collaboration [68,69,71]. Only statistical error bars are shown.

using $\kappa = 2$ GeV/fm. In contrast, an increase of effective string tension value to $\kappa = 5$ GeV/fm better describes classes with HM events. The remark is true for strange $\Lambda + \bar{\Lambda}$ as well as for multistrange ($\Xi^- + \bar{\Xi}^+$, $\Omega^- + \bar{\Omega}^+$) particles in pp collisions at $\sqrt{s} = 7$ TeV.

To conclude, for a better description of (multi)strange particle productions in high charged-particle multiplicity pp collisions, we have to consider an increase of effective string tension value from $\kappa = 2$ to $\kappa = 5$ GeV/fm, is strongly supported by data. The fact that an effective value $\kappa = 5$ GeV/fm describes better the R_{mb} ratio in pp collisions at $\sqrt{s} = 7$ TeV reveals features similar to those observed in chromoelectric flux configurations used to describe some experimental observables in Pb-Pb collisions at $\sqrt{s_{NN}} = 2.76$ TeV [60]. The enhancement of (multi)strange hadron yields as function of multiplicity has been associated with the creation of a strongly interacting medium, sQGP [88]. Recently, a similar behavior was also observed for multistrange hadrons in high-multiplicity pp collisions [8] and this observation challenges all string fragmentation models [10]. Finally, we remark that for pp collisions at $\sqrt{s} = 7$ TeV our model predicts higher sensitivity to SLCF effects for ID (multi)strange (Λ , Ξ , Ω) than for light hadrons (π , K , p). The calculations assuming an effective string tension value which vary only with energy as $\kappa(s) = \kappa_0 (s/s_0)^{0.04}$ GeV/fm describe fairly well the (multi)strangeness production in the LM event classes, but fail to describe (multi)strange production in HM event classes. A

better description is obtained for an enhanced effective string tension value $\kappa = 5$ GeV/fm which points to the necessity of a new dependency on multiplicity (or ϵ_{ini}) for the effective string tension value.

IV. SUMMARY AND CONCLUSIONS

In summary, we studied in the framework of the HIJING/ $B\bar{B}$ v2.0 model, the influence of possible strong homogeneous constant color electric fields on new experimental observables measured by the ALICE Collaboration, especially for identified particles in pp , p -Pb, and Pb-Pb collisions at $\sqrt{s} = 7$ TeV, $\sqrt{s_{NN}} = 5.02$ TeV, and $\sqrt{s_{NN}} = 2.76$ TeV, respectively. The effective string tension κ controls $Q\bar{Q}$ pair creation rates and the suppression factors $\gamma_{Q\bar{Q}}$. The measured average transverse momentum and ratio R_{mb} of ID particle help to verify our assumptions and to set the strangeness suppression factor. We assume in our calculations energy and possible system dependences of the effective string tension, κ .

For Pb-Pb collisions at $\sqrt{s_{NN}} = 2.76$ TeV, all nuclear effects included in the model, e.g., strong color fields, shadowing and quenching should be taken into account. However, partonic energy loss and jet quenching process, as embedded in the model, brought a fair description of the p_T distributions of identified light hadrons (π , K , p). The discrepancy could be explained by an initial condition with large pressure and

therefore a large collective flow, which is not embedded in our model.

For identified particle in pp collisions at $\sqrt{s} = 7$ TeV, we compute correlation between mean transverse momentum and multiplicity of charged particles (N_{ch}^*) at central rapidity as well as the ratio of double differential cross sections normalized to the charged particle densities versus multiplicity, R_{mb} . In the calculations, we take into account the variation of strong color (electric) fields with energy but not with the multiplicity (or initial energy densities, ϵ_{ini}) of the colliding system. The assumed effective string tension is $\kappa = 2$ GeV/fm, corresponding to $\kappa(s) = \kappa_0 (s/s_0)^{0.04}$ GeV/fm [see Eq. (4)]. Since we expect in high-multiplicity proton-proton collisions features that are similar to those observed in Pb-Pb collisions, we consider also the results obtained with an enhanced value of the effective string tension, from $\kappa = 2$ to $\kappa = 5$ GeV/fm. This increase of the strength of color fields leads to a ratio R_{mb} consistent with recent data for the HM class of events, while the LM class of events is better described using a lower effective string tension value of $\kappa = 2$ GeV/fm. These results show that the above increase of the strength of color fields could be an important dynamical mechanisms. New

measurements with high statistics at low and intermediate p_T ($1 < p_T < 6$ GeV/ c) of the ratio R_{mb} in pp collisions at LHC energies could help to disentangle different model approaches and/or different dynamical mechanisms, especially for high-multiplicity event classes.

Note that the HIJING/ $B\bar{B}$ model is based on a time-independent strength of color field, while in reality the production of $Q\bar{Q}$ pairs is a time- and space-dependent phenomenon, being far from equilibrium. To achieve more quantitative conclusions, such time- and space-dependent mechanisms [28,73] should be considered in the next generation of Monte Carlo codes.

ACKNOWLEDGMENTS

V.T.P. would like to acknowledge useful discussions with Miklos Gyulassy and Jean Barrette in the early phase of analysis. This work was supported by the Ministry of Research and Innovation via CNCSI and IFA coordinating agencies Projects number 44/05.10.2011 and 4/16.03.2016, and in part by Natural Sciences and Engineering Research Council of Canada.

-
- [1] V. Khachatryan *et al.* (CMS Collaboration), *J. High Energy Phys.* **1009**, 091 (2010).
- [2] S. Chatrchyan *et al.* (CMS Collaboration), *Phys. Lett. B* **718**, 795 (2013).
- [3] B. Abelev *et al.* (ALICE Collaboration), *Phys. Lett. B* **719**, 29 (2013).
- [4] G. Aad *et al.* (ATLAS Collaboration), *Phys. Lett. B* **725**, 60 (2013).
- [5] C. Andrei (ALICE Collaboration), *Nucl. Phys. A* **931**, 888 (2014).
- [6] G. Aad *et al.* (ATLAS Collaboration), *Phys. Rev. Lett.* **116**, 172301 (2016).
- [7] M. Witek (LHCb Collaboration), *EPJ Web Conf.* **141**, 01007 (2017).
- [8] J. Adam *et al.* (ALICE Collaboration), *Nat. Phys.* **13**, 535 (2017).
- [9] S. Schlichting and P. Tribedy, *Adv. High Energy Phys.* **2016**, 8460349 (2016).
- [10] N. Fischer and T. Sjöstrand, *J. High Energy Phys.* **01** (2017) 140.
- [11] C. Bierlich, G. Gustafson, and L. Lönnblad, *Phys. Lett. B* **779**, 58 (2018).
- [12] T. Pierog, I. Karpenko, J. M. Katzy, E. Yatsenko, and K. Werner, *Phys. Rev. C* **92**, 034906 (2015).
- [13] K. Werner, B. Guiot, I. Karpenko, and T. Pierog, *Phys. Rev. C* **89**, 064903 (2014).
- [14] K. Werner, B. Guiot, I. Karpenko, and T. Pierog, *Nucl. Phys. A* **931**, 83 (2014).
- [15] M. Petrovici, I. Berceanu, A. Pop, M. Târziă, and C. Andrei, *Phys. Rev. C* **96**, 014908 (2017).
- [16] J. S. Schwinger, *Phys. Rev.* **82**, 664 (1951).
- [17] T. S. Biro, H. B. Nielsen, and J. Knoll, *Nucl. Phys. B* **245**, 449 (1984).
- [18] A. Bialas and W. Czyz, *Phys. Rev. D* **31**, 198 (1985).
- [19] M. Gyulassy and A. Iwazaki, *Phys. Lett. B* **165**, 157 (1985).
- [20] C. Merino, C. Pajares, and J. Ranft, *Phys. Lett. B* **276**, 168 (1992).
- [21] N. Tanji, *Ann. Phys.* **324**, 1691 (2009).
- [22] R. Ruffini, G. Vereshchagin, and S.-S. Xue, *Phys. Rept.* **487**, 1 (2010).
- [23] L. Labun and J. Rafelski, *Phys. Rev. D* **79**, 057901 (2009).
- [24] N. Cardoso, M. Cardoso, and P. Bicudo, *Phys. Lett. B* **710**, 343 (2012).
- [25] G. C. Nayak, *Phys. Rev. D* **72**, 125010 (2005).
- [26] G. C. Nayak and P. van Nieuwenhuizen, *Phys. Rev. D* **71**, 125001 (2005).
- [27] P. Levai and V. Skokov, *J. Phys. G* **36**, 064068 (2009).
- [28] P. Levai and V. Skokov, *Phys. Rev. D* **82**, 074014 (2010).
- [29] P. Levai and V. V. Skokov, *AIP Conf. Proc.* **1348**, 118 (2011).
- [30] P. Levai, D. Berenyi, A. Pasztor, and V. V. Skokov, *J. Phys. G* **38**, 124155 (2011).
- [31] B. Andersson, G. Gustafson, G. Ingelman, and T. Sjöstrand, *Phys. Rept.* **97**, 31 (1983).
- [32] X.-N. Wang and M. Gyulassy, *Phys. Rev. Lett.* **68**, 1480 (1992); *Phys. Rev. D* **44**, 3501 (1991).
- [33] X. N. Wang and M. Gyulassy, *Phys. Lett. B* **282**, 466 (1992).
- [34] F. Gelis, T. Lappi, and L. McLerran, *Nucl. Phys. A* **828**, 149 (2009); T. Lappi and L. McLerran, *ibid.* **772**, 200 (2006).
- [35] L. McLerran, *J. Phys. G* **35**, 104001 (2008).
- [36] D. Kharzeev, E. Levin, and K. Tuchin, *Phys. Rev. C* **75**, 044903 (2007).
- [37] M. A. Braun, C. Pajares, and V. V. Vechernin, *Nucl. Phys. A* **906**, 14 (2013).
- [38] H. Sorge, M. Berenguer, H. Stoecker, and W. Greiner, *Phys. Lett. B* **289**, 6 (1992).
- [39] S. A. Bass *et al.*, *Prog. Part. Nucl. Phys.* **41**, 255 (1998).
- [40] M. Bleicher *et al.*, *J. Phys. G* **25**, 1859 (1999).
- [41] S. Soff, D. Zschesche, M. Bleicher, C. Hartnack, M. Belkacem, L. Bravina, E. Zabrodin, S. A. Bass, H. Stoecker, and W. Greiner, *J. Phys. G* **27**, 449 (2001).

- [42] S. Soff, J. Randrup, H. Stoecker, and N. Xu, *Phys. Lett. B* **551**, 115 (2003).
- [43] Z. W. Lin, C. M. Ko, B. A. Li, B. Zhang, and S. Pal, *Phys. Rev. C* **72**, 064901 (2005).
- [44] M. A. Braun, J. Dias de Deus, A. S. Hirsch, C. Pajares, R. P. Scharenberg, and B. K. Srivastava, *Phys. Rept.* **599**, 1 (2015).
- [45] I. Bautista Guzman, R. Alvarado, and P. Fierro, *PoS ICHEP2016*, 1152 (2017).
- [46] C. Merino, C. Pajares, M. M. Ryzhinskiy, Y. M. Shabelski, and A. G. Shuvaev, *Phys. Atom. Nucl.* **73**, 1781 (2010); **74**, 173 (2011)].
- [47] I. Bautista and C. Pajares, *Phys. Rev. C* **82**, 034912 (2010).
- [48] C. Bierlich, G. Gustafson, L. Lönnblad, and A. Tarasov, *J. High Energy Phys.* **03** (2015) 148.
- [49] C. Bierlich and J. R. Christiansen, *Phys. Rev. D* **92**, 094010 (2015).
- [50] G. Feofilov, V. Kovalenko, and A. Puchkov, [arXiv:1710.08895](https://arxiv.org/abs/1710.08895) [hep-ph].
- [51] E. O. Bodnya, V. N. Kovalenko, A. M. Puchkov, and G. A. Feofilov, *AIP Conf. Proc.* **1606**, 273 (2014).
- [52] N. Armesto, D. A. Derkach, and G. A. Feofilov, *Phys. At. Nucl.* **71**, 2087 (2008).
- [53] W.-T. Deng, X.-N. Wang, and R. Xu, *Phys. Rev. C* **83**, 014915 (2011).
- [54] W.-T. Deng, X.-N. Wang, and R. Xu, *Phys. Lett. B* **701**, 133 (2011).
- [55] V. Topor Pop, M. Gyulassy, J. Barrette, C. Gale, X. N. Wang, and N. Xu, *Phys. Rev. C* **70**, 064906 (2004).
- [56] V. Topor Pop, M. Gyulassy, J. Barrette, and C. Gale, *Phys. Rev. C* **72**, 054901 (2005).
- [57] V. Topor Pop, M. Gyulassy, J. Barrette, C. Gale, S. Jeon, and R. Bellwied, *Phys. Rev. C* **75**, 014904 (2007).
- [58] V. Topor Pop, J. Barrette, and M. Gyulassy, *Phys. Rev. Lett.* **102**, 232302 (2009).
- [59] V. Topor Pop, M. Gyulassy, J. Barrette, C. Gale, and A. Warburton, *Phys. Rev. C* **83**, 024902 (2011).
- [60] V. Topor Pop, M. Gyulassy, J. Barrette, C. Gale, and M. Petrovici, *J. Phys. G* **41**, 115101 (2014).
- [61] V. Topor Pop, M. Gyulassy, J. Barrette, and C. Gale, *Phys. Rev. C* **84**, 044909 (2011).
- [62] G. G. Barnafoldi, J. Barrette, M. Gyulassy, P. Levai, and V. Topor Pop, *Phys. Rev. C* **85**, 024903 (2012).
- [63] V. Topor Pop, M. Gyulassy, J. Barrette, C. Gale, and A. Warburton, *Phys. Rev. C* **86**, 044902 (2012).
- [64] J. L. Albacete, N. Armesto, R. Baier, G. G. Barnafoldi, J. Barrette, S. De, W.-T. Deng, and A. Dumitru *et al.*, *Int. J. Mod. Phys. E* **22**, 1330007 (2013).
- [65] J. L. Albacete *et al.*, *Int. J. Mod. Phys. E* **25**, 1630005 (2016).
- [66] G. Ripka (ed.), *Dual Superconductor Models of Color Confinement*, Lecture Notes in Physics (Springer, Berlin, Heidelberg, 2004), Vol. 639.
- [67] V. K. Magas, L. P. Csernai, and D. Strottman, *Nucl. Phys. A* **712**, 167 (2002).
- [68] L. Bianchi (ALICE Collaboration), *Nucl. Phys. A* **956**, 777 (2016).
- [69] R. Derradi de Souza (ALICE Collaboration), *J. Phys. Conf. Ser.* **779**, 012071 (2017).
- [70] V. Vislavicius (ALICE Collaboration), *Nucl. Phys. A* **967**, 337 (2017).
- [71] S. Acharya *et al.* (ALICE Collaboration), [arXiv:1807.11321](https://arxiv.org/abs/1807.11321) [nucl-ex].
- [72] T. D. Cohen and D. A. McGady, *Phys. Rev. D* **78**, 036008 (2008).
- [73] F. Hebenstreit, R. Alkofer, and H. Gies, *Phys. Rev. D* **78**, 061701 (2008).
- [74] Particle Data Group, K. Nakamura *et al.*, *J. Phys. G* **37**, 075021 (2010).
- [75] M. Cristoforetti, P. Faccioli, G. Ripka, and M. Traini, *Phys. Rev. D* **71**, 114010 (2005).
- [76] N. S. Amelin, N. Armesto, C. Pajares, and D. Sousa, *Eur. Phys. J. C* **22**, 149 (2001).
- [77] L. McLerran and M. Praszalowicz, *Acta Phys. Polon. B* **41**, 1917 (2010).
- [78] KAamodt *et al.* (ALICE Collaboration), *Phys. Rev. Lett.* **105**, 252301 (2010).
- [79] B. Abelev *et al.* (ALICE Collaboration), *Phys. Rev. Lett.* **110**, 032301 (2013).
- [80] B. Andersson, G. Gustafson, and B. Nilsson-Almqvist, *Nucl. Phys. B* **281**, 289 (1987); B. Nilsson-Almqvist and E. Stenlund, *Comput. Phys. Commun.* **43**, 387 (1987).
- [81] H.-U. Bengtsson and T. Sjöstrand, *Comput. Phys. Commun.* **46**, 43 (1987).
- [82] T. Sjöstrand, S. Mrenna, and P. Z. Skands, *J. High Energy Phys.* **05** (2006) 026.
- [83] B. B. Abelev *et al.* (ALICE Collaboration), *Phys. Lett. B* **727**, 371 (2013).
- [84] J. Liao and E. Shuryak, *Phys. Rev. D* **82**, 094007 (2010).
- [85] O. Kaczmarek and F. Zantow, *Phys. Rev. D* **71**, 114510 (2005).
- [86] E. Shuryak, [arXiv:1806.10487](https://arxiv.org/abs/1806.10487).
- [87] T. Alexopoulos *et al.*, *Phys. Rev. Lett.* **64**, 991 (1990).
- [88] B. B. Abelev *et al.* (ALICE Collaboration), *Phys. Lett. B* **728**, 25 (2014).
- [89] J. D. Bjorken, Preprint FERMILAB-PUB-82/59-THY (1982).
- [90] L. Van Hove, *Phys. Lett. B* **118**, 138 (1982).
- [91] R. Campanini and G. Ferri, *Phys. Lett. B* **703**, 237 (2011).
- [92] B. B. Abelev *et al.* (ALICE Collaboration), *Phys. Lett. B* **736**, 196 (2014).
- [93] J. Adam *et al.* (ALICE Collaboration), *Eur. Phys. J. C* **75**, 226 (2015).
- [94] S. Chatrchyan *et al.* (CMS Collaboration), *Eur. Phys. J. C* **72**, 2164 (2012).
- [95] M. Petrovici, A. Lindner, A. Pop, M. Târziã, and I. Berceanu, *Phys. Rev. C* **98**, 024904 (2018).